Circadian rhythms synchronize mitosis in *Neurospora crassa*

Christian I. Hong[a,1], Judit Zámborszky[a], Mokryun Baek[a], Laszlo Labiscsak[a], Kyungsu Ju[a], Hyeyeong Lee[a], Luis F. Larrondo[b], Alejandra Goity[b], Hin Siong Chong[c], William J. Belden[c], and Attila Csikász-Nagy[d,e]

[a]Department of Molecular and Cellular Physiology, University of Cincinnati, Cincinnati, OH 45267; [b]Departamento de Genética Molecular y Microbiología, Facultad de Ciencias Biológicas, Pontificia Universidad Católica de Chile, Casilla 114-D, Santiago, Chile; [c]Department of Biochemistry and Microbiology, Rutgers, The State University of New Jersey, New Brunswick, NJ 08901; [d]Randall Division of Cell and Molecular Biophysics and Institute for Mathematical and Molecular Biomedicine, King's College London, London SE1 UL, United Kingdom; and [e]Department of Computational Biology, Research and Innovation Centre, Fondazione Edmund Mach, 38010 San Michele all'Adige, Italy

Edited* by Jay C. Dunlap, Geisel School of Medicine at Dartmouth, Hanover, NH, and approved December 11, 2013 (received for review October 15, 2013)

The cell cycle and the circadian clock communicate with each other, resulting in circadian-gated cell division cycles. Alterations in this network may lead to diseases such as cancer. Therefore, it is critical to identify molecular components that connect these two oscillators. However, molecular mechanisms between the clock and the cell cycle remain largely unknown. A model filamentous fungus, *Neurospora crassa*, is a multinucleate system used to elucidate molecular mechanisms of circadian rhythms, but not used to investigate the molecular coupling between these two oscillators. In this report, we show that a conserved coupling between the circadian clock and the cell cycle exists via serine/threonine protein kinase-29 (STK-29), the Neurospora homolog of mammalian WEE1 kinase. Based on this finding, we established a mathematical model that predicts circadian oscillations of cell cycle components and circadian clock-dependent synchronized nuclear divisions. We experimentally demonstrate that G1 and G2 cyclins, CLN-1 and CLB-1, respectively, oscillate in a circadian manner with bioluminescence reporters. The oscillations of *clb-1* and *stk-29* gene expression are abolished in a circadian arrhythmic *frq*^{ko} mutant. Additionally, we show the light-induced phase shifts of a core circadian component, *frq*, as well as the gene expression of the cell cycle components *clb-1* and *stk-29*, which may alter the timing of divisions. We then used a histone hH1-GFP reporter to observe nuclear divisions over time, and show that a large number of nuclear divisions occur in the evening. Our findings demonstrate the circadian clock-dependent molecular dynamics of cell cycle components that result in synchronized nuclear divisions in Neurospora.

Molecular mechanisms of circadian rhythms provide temporal information to other cellular processes, such as metabolism, to optimize their outcomes (1–3). For instance, circadian oscillations of rate-limiting genes in glucose metabolism suggest time-of-day specific regulatory mechanisms that maintain glucose homeostasis in mammals (3). Circadian clock-gated cell division cycles have been observed in various organisms, including mammals, indicating that cell divisions preferentially occur at specific times of the day (4–7). In the mouse liver, expression of the cell cycle kinase-encoding gene, *wee1*, is directly activated by a heterodimeric circadian transcription factor, CLOCK-BMAL1, providing a molecular link between the cell cycle and circadian rhythms (5). This suggests that circadian clock-regulated WEE1 promotes periodic inhibition of mitotic cycles between G2 and M phase by phosphorylating and inactivating the mitotic cyclin-dependent kinase (CDK) (8). On the other hand, circadian-independent cell divisions have been reported in rat-1 fibroblasts despite the fact that these cells maintain robust circadian rhythms (9). These data suggest that not all cells with circadian rhythms may display circadian-gated cell division cycles.

The multinucleate fungus *Neurospora crassa* has played a pivotal role in elucidating the molecular mechanism of circadian rhythms (10, 11). Briefly, circadian rhythms in *N. crassa* are regulated by positive and negative elements that create a time-delayed negative feedback loop (12). A heterodimeric transcription factor, White Collar Complex (WCC, which consists of WC-1 and WC-2), activates transcription of the *frequency* (*frq*) gene. Its product, FRQ protein, interacts with an RNA helicase, FRH (13), and inactivates the WCC by indirectly phosphorylating and removing WCC from the nucleus (14–16). FRQ is phosphorylated progressively over time, which makes it more susceptible to ubiquitination and degradation triggered by its conformational changes (17–19). The degradation of FRQ results in a new cycle of transcriptional activations by the WCC.

Previous studies in Neurospora showed asynchronous mitotic divisions, with no report of circadian-gated division cycles, despite the presence of robust circadian rhythms (20–22). On the other hand, although synchronous nuclear divisions are observed in other fungi, such as *Aspergillus nidulans*, it is unknown whether circadian rhythms play a role in the synchrony of their divisions (23). Recent use of GFP labeling has facilitated detailed observations of mitosis in germinating conidia, supporting models for asynchronous mitotic nuclear divisions (21, 24). These experiments, however, did not take into account the potential influence of circadian rhythms in mitotic division cycles. In Neurospora, robust circadian oscillations are observed in constant darkness (DD) or under entrainment regimens (e.g., light–dark cycles), but not in constant light (LL) conditions. There are no reports of experiments that address functional roles of circadian rhythms in mitotic divisions in the syncytium system.

Significance

Circadian rhythms provide temporal information to other cellular processes, such as metabolism. We investigate the coupling between the cell cycle and the circadian clock using mathematical modeling and experimentally validate model-driven predictions with a model filamentous fungus, *Neurospora crassa*. We demonstrate a conserved coupling mechanism between the cell cycle and the circadian clock in Neurospora as in mammals, which results in circadian clock-gated mitotic cycles. Furthermore, we observe circadian clock-dependent phase shifts of G1 and G2 cyclins, which may alter the timing of divisions. Our work has large implications for the general understanding of the connection between the cell cycle and the circadian clock.

Author contributions: C.I.H. and A.C.-N. designed research; J.Z., M.B., L.L., K.J., H.L., L.F.L., A.G., H.S.C., and W.J.B. performed research; J.Z. performed mathematical modeling; C.I.H., J.Z., and A.C.-N. analyzed data; and C.I.H., J.Z., L.F.L., W.J.B., and A.C.-N. wrote the paper.

The authors declare no conflict of interest.

*This Direct Submission article had a prearranged editor.

Freely available online through the PNAS open access option.

[1]To whom correspondence should be addressed. E-mail: christian.hong@uc.edu.

This article contains supporting information online at www.pnas.org/lookup/suppl/doi:10.1073/pnas.1319399111/-/DCSupplemental.

The cell cycle regulation of Neurospora has yet to be investigated thoroughly because of some technical limitations, such as adequate methods to synchronize, image, and measure doubling times of nuclear divisions in growing mycelia. We explored the Neurospora genome (25) to find the homologs of key cell cycle regulators and found that Neurospora has a low number of predicted cyclins and CDKs. Neurospora has a single *Cdk1* homolog (*cdc-2*, NCU09778), one G1 cyclin that resembles the sequence of the G1/S regulating budding yeast *Clns* (*cln-1*, NCU02114), and two B-type cyclins (*clb-1*, NCU02758, and *clb-3*, NCU01242) (26). There also exists a homolog of the CDK1 inhibitor WEE1 kinase (*stk-29*, NCU04326), which is regulated in a circadian manner in the mouse liver (5). Interactions between the above homologous proteins in budding and fission yeast have been well characterized, and their conservation among eukaryotes (27, 28) suggests they may be wired in a similar fashion in *N. crassa*.

Here, we investigate the molecular connection between the cell cycle and the circadian clock and functional consequences of this coupling in *N. crassa*. First, we show that there is a conserved connection between the cell cycle and the circadian clock in Neurospora as in mammals via STK-29, which is the Neurospora homolog of WEE1. Based on this finding and on the hypothesis of conserved cell cycle regulatory interactions, we use mathematical modeling to investigate molecular profiles of both cell cycle and circadian clock components. Our computational simulations predict circadian oscillations of cell cycle components, such as CLN-1 and CLB-1. We experimentally validate this prediction with luciferase bioluminescence reporters to track both cell cycle and circadian clock components in real time in vivo. Moreover, we demonstrate circadian clock-induced phase shifts of cell cycle components, which may alter the timing of divisions. The circadian oscillations of key cell cycle components suggest circadian clock-gated synchronized nuclear divisions. By observing nuclear morphology over time at 25 °C in DD, we indicate that most divisions occur in the evening. We propose that there is a significant coupling between the cell cycle and the circadian clock, which might result in immediate changes in the dynamics of cell cycle regulation upon alterations in circadian rhythms.

Results

There Is a Conserved Coupling Between the Cell Cycle and the Circadian Clock in *N. crassa* as in *Mus musculus*. A heterodimeric circadian transcription factor, WCC, recognizes light-responsive elements (LREs) to activate target genes (13, 29, 30). We found four putative LREs (GAGATCC, CCGATCC, CCGATCG, and TCGATCT) within 1.75 kb of the *stk-29* gene 5′ upstream region (Fig. 1*A*). To test WCC-dependent activation of *stk-29*, we performed a light induction experiment. WC-1 is also a photoreceptor that undergoes a light induction response, which is described by a sharp increase in its expression followed by a decrease to its basal level of expression when Neurospora is transferred from dark to light conditions (Fig. 1*B*). Light-induced WC-1 activates many downstream target genes by recognizing LREs (31). We observe light response from *stk-29* mRNA in the wild type, which is abolished in the *wc-1*^{ko} (Fig. 1 *C* and *D*). In contrast, we do not observe a light response of *cln-1* mRNA in wild-type strains (Fig. 1*E*). The WC-1–dependent light response of *stk-29* indicates that *stk-29* is activated by WCC and that it is a potential target for circadian regulation. To verify direct binding of WCC to the promoter of *stk-29*, we performed a WC-2 ChIP experiment and show that the WC-2 binds to the region close to LRE1 (Fig. 1*F*). Based on the finding that *stk-29* is activated by WCC, we tested a mathematical model of the Neurospora circadian clock and cell cycle as a coupled oscillator and explored coupled dynamics (Figs. S1–S4 and Tables S1–S5).

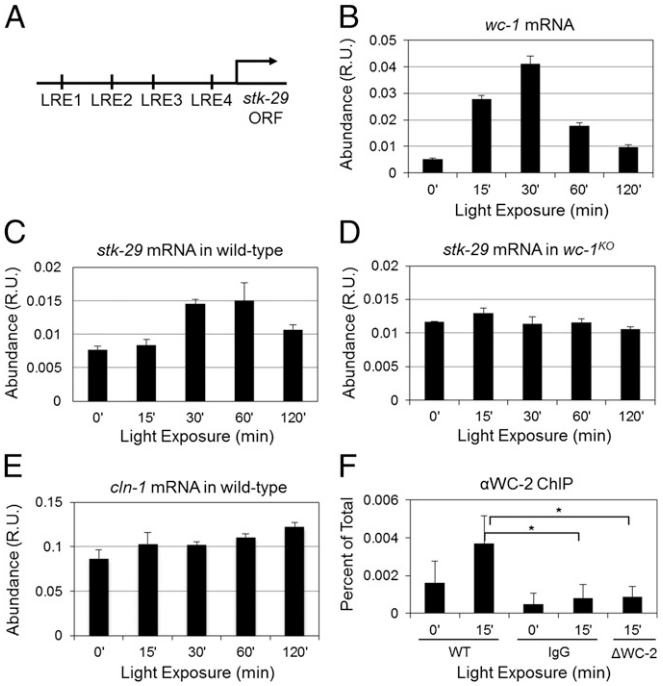

Fig. 1. *stk-29* mRNA shows WC-1–dependent light response, and WC-2 directly binds to the *stk-29* promoter. (*A*) There are four LREs within 1.75 kb of the *stk-29* gene 5′ upstream region. The first LRE, GAGATCC, is located ∼1.75 kb upstream (LRE1); the second LRE, CCGATCC, is located ∼1.2 kb upstream (LRE2); the third LRE, CCGATCG, is located ∼0.8 kb upstream (LRE3); and the fourth LRE, TCGATCT, is located ∼0.25 kb upstream (LRE4) of the *stk-29* gene. (*B*) *wc-1* mRNA undergoes light response when Neurospora is moved from dark to light conditions. (*C* and *D*) *stk-29* mRNA shows light response in the wild type (*C*), which is abolished in *wc-1*^{ko} (*D*). (*E*) *cln-1* mRNA does not show light response in the wild type. The above data are relative units (R.U.) normalized with *actin* mRNA. The average ± SD is shown. The above data are representative of two or more independent experiments. (*F*) WC-2 directly binds to the promoter of *stk-29*. ChIP assay was performed on a wild-type strain (FGSC2489), with samples grown in the dark (0′) or in response to a 15-min light pulse (15′) using a polyclonal antibody that recognizes WC-2 protein and oligos specific for a region of the *stk-29* promoter. A nonspecific IgG and a strain lacking the *wc-2* gene (*Δwc-2*) were used as controls. The results are an average of five experiments, and the error bars represent the SDs. The asterisks indicate a *P* value <0.001.

***cln-1* and *clb-1* Gene Expression and Protein Abundance Show Circadian Clock-Dependent Oscillations.** Our mathematical model predicts circadian oscillations of cell cycle components such as CLN-1 and CLB-1 proteins if intermediate to strong coupling exists between the circadian clock and the cell cycle (Figs. S1–S4). To validate circadian-dependent oscillations of cell cycle factors, we constructed bioluminescence reporters to track in vivo gene expression of *cln-1* (NCU02114), *clb-1* (NCU02758), *stk-29* (NCU04326), and *cdc-2* (NCU09778) in real time. Bioluminescence reporters were constructed by fusing the fully codon-optimized luciferase from firefly with a promoter of interest (32). Our data indicate that expression of *cln-1*, *clb-1*, and *stk-29* from populations of Neurospora nuclei show circadian oscillations (Fig. 2*A*). We also observe circadian oscillations of *cln-1* and *clb-1* mRNA expressions (Fig. S5). Expression of *cdc-2*, however, does not follow circadian regulation (Fig. 2*A*). This is in accord with the cell cycle model that we adapted (33), which assumes constitutive expression of *cdc-2*. We then constructed translational bioluminescence reporters of CLN-1^{luc}, CLB-1^{luc}, and CDC-2^{luc} by fusing luciferase to genes of interest as previously described for FRQ^{luc} (34), and followed protein abundances of CLN-1, CLB-1, and CDC-2. The abundance of both CLN-1 and CLB-1

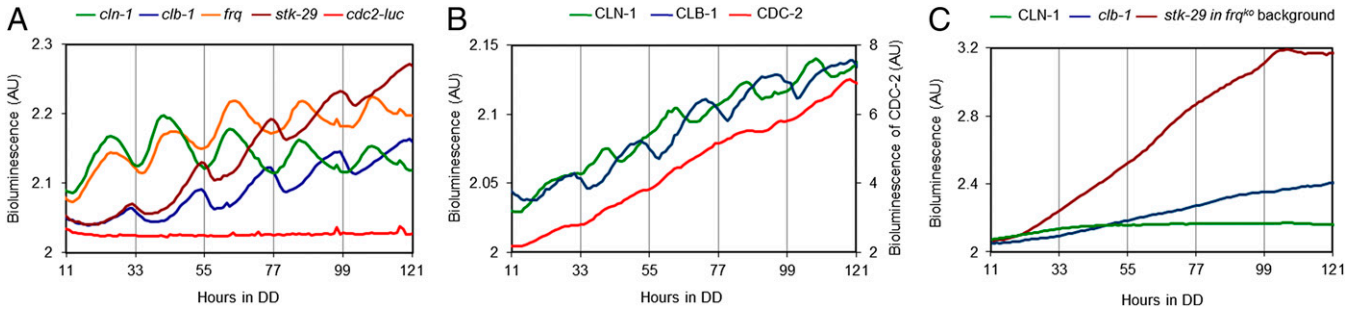

Fig. 2. *cln-1*, *clb-1*, and *stk-29* demonstrate circadian oscillations. (*A*) *cln-1*, *clb-1*, *stk-29*, and *cdc-2* promoters are fused to the codon-optimized firefly luciferase (32) for real-time analyses of their gene expressions in vivo. A strain carrying *frq-luciferase* reporter, an established core circadian component, is used as a positive control. (*B*) *cln-1*, *clb-1*, and *cdc-2* genes are fused with the codon-optimized firefly luciferase for real-time observation of CLN-1, CLB-1, and CDC-2 protein abundances. (*C*) A strain housing *clb-1–luciferase* or *stk-29–luciferase* reporter is crossed with frq^{ko} mutant resulting in *clb-1–luciferase* and *stk-29–luciferase* reporters in frq^{ko} background that show loss of circadian oscillations of *clb-1* and *stk-29* gene expression. Similarly, the CLN-1^{luc} translational reporter is crossed with frq^{ko} mutant, resulting in a CLN-1^{luc} reporter strain in frq^{ko} background, which shows an arrhythmic phenotype. The above data are representative of three or more independent experiments. Arbitrary units (AU) are shown.

shows circadian oscillations with phase information similar to that of their gene expression profiles (Fig. 2*B*). The observed phase relationship between CLN-1 and CLB-1 is expected based on their cell cycle functions in G1 and G2/M phases, respectively. In contrast, the abundance of CDC-2 increases continuously over time, corresponding to the growth in mass of Neurospora, and does not exhibit circadian oscillations (Fig. 2*B*). The data suggest that CDC-2 is stable with a constant rate of expression, consistent with findings in budding yeast (35). Importantly, circadian oscillations of CLN-1 protein and *clb-1* and *stk-29* gene expression are lost in the frq^{ko} strain, an arrhythmic mutant in which the circadian clock is nonfunctional (Fig. 2*C*). This indicates that the synchronized oscillations of cell cycle elements are under the influence of circadian rhythms.

Based on the above data, we hypothesized that the expression of cell cycle genes such as *clb-1* might be altered in a circadian manner. We performed light-pulse experiments to phase-shift circadian rhythms and investigated the circadian-dependent phase shifts of cell cycle components. We tracked bioluminescence of *frq*, *clb-1*, and *stk-29* gene expression after a 90-min light pulse at specific time points in DD. We observed ~3–5-h phase advances and delays in the expression of *frq*, *clb-1*, and *stk-29* when light pulses were given at DD32 [circadian time 23 (CT23)] and DD48 (CT16), respectively (Fig. 3). This demonstrates that the phases of *clb-1* and *stk-29* gene expression are influenced by phase

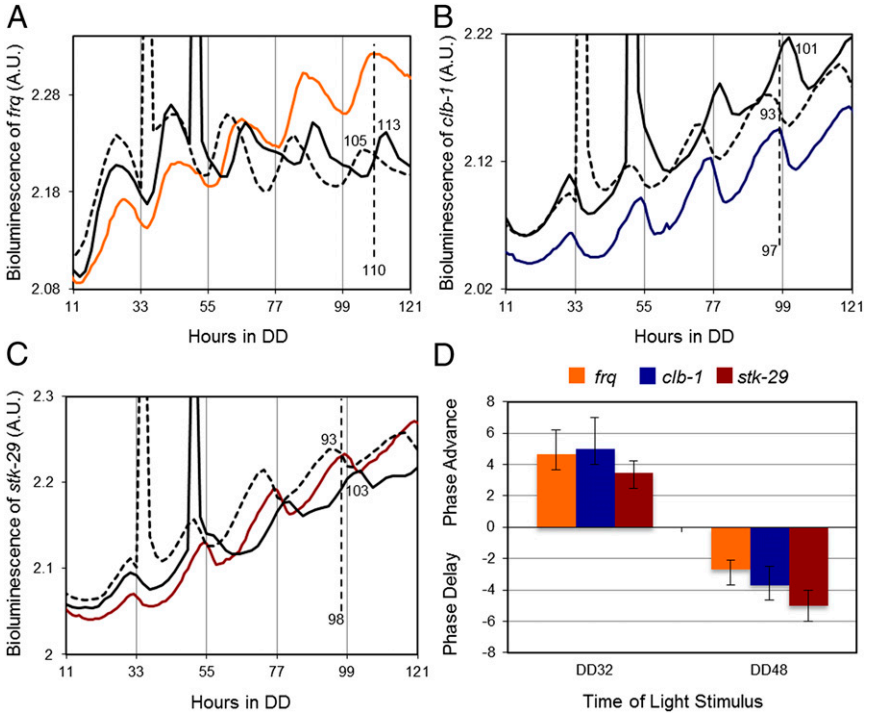

Fig. 3. *clb-1* and *stk-29* gene expressions indicate circadian clock-dependent phase shifts. (*A*–*C*) A 90-min light pulse is given at either DD32 (dashed black) or DD48 (solid black), and the phases of peak expressions of *frq*, *clb-1*, and *stk-29* genes are compared with unperturbed data (*frq*, orange; *clb-1*, blue; *stk-29*, maroon) at the fourth peak of unperturbed data (dashed straight line). Corresponding peaks are labeled in each figure. The data shown represent three independent experiments. (*D*) A 90-min light stimulus at DD32 and DD48 creates ~3–5-h phase advances and delays, respectively. The data are from three independent experiments (Fig. S6), and the average ± SD is shown. Arbitrary units (AU) are shown.

changes of the circadian clock that are similar in degree and direction, which may alter the timing of nuclear divisions in *N. crassa*.

Circadian Clock-Dependent Synchronized Nuclear Divisions Occur in the Middle of the Night. The lack of circadian oscillations of *clb-1* gene expression in frq^{ko} does not necessarily indicate altered mitosis (Fig. 2*C*). Rather, it suggests asynchronous mitotic divisions uncoupled from circadian rhythms. To verify this, we investigated circadian clock-dependent synchronized nuclear divisions. In Neurospora, nuclei are visualized readily by using an *hH1-sgfp* strain in which histone H1 is fused to GFP (21, 24). By using this strain, the stages of the cell cycle can be visualized and categorized. We performed a time-course experiment under circadian conditions (i.e., DD at 25 °C) and classified the populations of nuclei into two categories: interphase and mitotic phase (Fig. 4*A*). At CT4, or during the subjective day, most nuclei are in interphase, as shown by round nuclear morphology (Fig. 4*B*). In contrast, many nuclei undergo mitosis at around CT17, which corresponds to late subjective evening (Fig. 4*C*). Although there is variability in mitotic stage, around 60% of nuclei are actively dividing in the evening (Fig. 4*D*). These data clearly demonstrate circadian oscillations in Neurospora mitotic divisions. The synchronized nuclear divisions are not observed in the frq^{ko} strain (Fig. 4*E*), which indicates that circadian rhythms are necessary for this daily synchronization of cell cycles. These observations are in accord with the arrhythmic *clb-1* and *stk-29* gene expression in frq^{ko} (Fig. 2*C*). We also used an established mitosis marker, phospho-histone H3 (pH3) antibody, as an independent measurement of mitosis (36, 37). We observed more pH3-positive nuclei at DD25 (CT15) than at DD35 (CT2) (Fig. S7 *A* and *B*).

The above experiments are performed by harvesting Neurospora from liquid culture media in DD and counting the number of nuclei present in fixed cells. It is important to note that we observe similar results via live cell imaging from Neurospora grown in defined solid agar media, in which we observe a second cycle of increased and decreased mitosis at DD47 and DD57, respectively (Fig. S8 and Movies S1–S4).

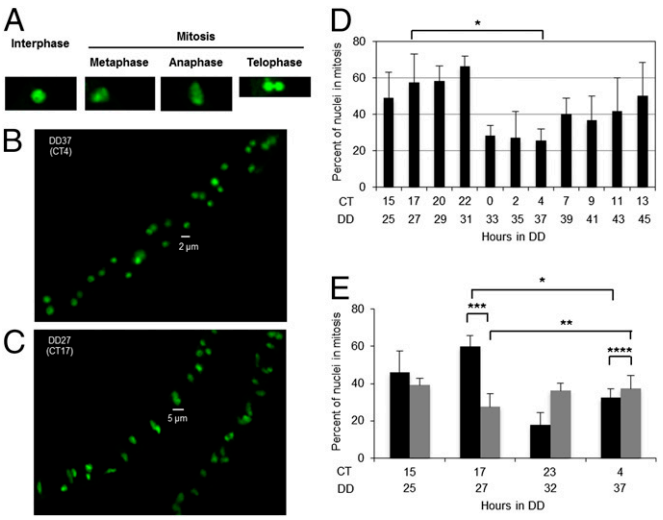

Fig. 4. Circadian clock-gated synchronized nuclear divisions are observed in Neurospora. (*A*) Different stages of mitotic cycles can be visualized with the *hH1-sgfp* strain and categorized based on the morphology of nuclei. (*B* and *C*) Microscopy data showing strands of hyphae at two different time points: CT4 and CT17. CT denotes circadian time in a free-running period in DD, in which subjective day begins at CT0 and subjective night begins at CT12. (*D*) Percentages of nuclei in mitosis are calculated as a time course with 2-h resolution. The average ± SD is shown. DD27 is statistically different from DD37 (*$P = 0.021$). The values are obtained from a time-course experiment with four to six samples from each time point. (*E*) Percentages of nuclei in mitosis are calculated and compared between the wild type (black) and frq^{ko} (gray) at four different time points (CT15, CT17, CT23, and CT4). The average ± SEM is shown. The data are from three or more independent experiments. Two-way ANOVA indicates there is a significant difference between DD27 and DD37 in the wild type (*$P = 0.012$) but not in the frq^{ko} strain (**$P = 0.33$). There is a significant difference between the wild type and the frq^{ko} at DD27 (***$P = 0.005$) but not at DD37 (****$P = 0.609$). Similar data are shown from live cell imaging (Fig. S8 and Movies S1–S4).

Discussion

In silico, we investigated various scenarios of coupled dynamics between the circadian clock and the cell cycle, which demonstrated circadian oscillations of cell cycle components if significant coupling exists between the two oscillators (Figs. S2–S4). We have demonstrated experimentally that elements of the cell cycle (e.g., *cln-1* and *clb-1*) undergo circadian oscillations, which manifest a circadian clock-dependent synchronized mitotic division in Neurospora. We also show that both *clb-1* and *stk-29* gene expression undergo light-dependent phase shifts in a length and direction similar to those of *frq* gene expression. This suggests circadian clock-dependent phase shifts of cell cycle components, which might be used to alter the timing of mitotic divisions.

The fundamental molecular regulatory architecture of circadian rhythms that highlight the time-delayed negative feedback mechanism is conserved from *N. crassa* to *M. musculus* (38). Coupling between circadian rhythms and the DNA damage response pathway is also conserved between Neurospora and mammals. Checkpoint kinase 2 (CHK2) is activated upon DNA damage and phosphorylates one of the core clock components (i.e., PER1 in mammals and FRQ in Neurospora), resulting in a subsequent degradation of PER1 or FRQ that leads to predominantly phase advances in circadian rhythms (39–43). We demonstrate that WC-2 binds to the promoter of *stk-29* (NCU04326) and that *stk-29* undergoes WC-1–dependent light-response and circadian oscillations, which shows conserved coupling between the cell cycle and circadian rhythms. The binding of WC-2 to the *stk-29* promoter was not reported in the recent WC-2 ChIP-sequencing data (44). This is probably a result of the low expression of *stk-29* and the less dramatic light response of *stk-29* compared with other targets. Further investigations are needed to understand the detailed dynamics of these connections as well as other possible coupling factors. We have shown circadian oscillations in a few cell cycle regulators. However, it is unclear whether these cycling components are genuine coupling components or mere reflections of the circadian-gated cell cycle determined by the currently known coupling factor STK-29. Recently, microarray data have suggested that several genes in cell cycle control show oscillatory behavior in Neurospora (45). Identification of other factors that couple the cell cycle and circadian rhythms will elucidate distinct points of interactions in which the circadian clock influences the cell cycle.

Identified conserved coupling components (i.e., CHK2 and WEE1) among the circadian clock, DNA damage response, and cell cycle mechanisms pose Neurospora as an ideal model organism to investigate the fundamental wiring of this network. However, one of the main disadvantages of Neurospora is that it is technically difficult to assess the doubling time of mitotic cycles in Neurospora mycelium grown on solid agar media. Previous measurements in liquid culture media showed a range in doubling time from 72 to 239 min, depending on growth conditions from young germinating conidia (46), which is in good agreement with our measurements in noncircadian conditions (e.g., LL) (Fig. S9). However, the doubling time in mature mycelium in circadian conditions (i.e., DD) might be different because of the presence of the circadian clock. Therefore, measuring the doubling time of nuclear divisions in DD for an extended period will be critical for future experiments. Real-time fluorescence and bioluminescence reporters, in addition to the use of

microfluidic devices for single-nucleus imaging, may facilitate measurement of doubling times for Neurospora growing in both liquid culture and solid agar media.

In this report, we demonstrate that many nuclear divisions occur during a specific window of circadian time. However, our experimental data also show that synchronized divisions are spread out over 6 h, with less frequent nuclear divisions also occurring at other times of the day (Fig. 4*D*). This does not imply that a single nucleus spends 6 h in the mitotic state; rather, our data suggest an increase in mitosis as a population within that 6-h window. It is also possible to hypothesize that a weak coupling might exist that enables the circadian clock to modulate the total abundance of CLB-1, which might allow more divisions during the evening in a threshold-dependent manner while keeping the cell cycle time short (Figs. S2*B* and S3*B*). Another hypothesis that might result in the observed phenotype is context-dependent (e.g., aging, nutrient conditions) weak to strong coupling. Our modeling work and other mathematical models predict quasi-periodic multimodal doubling times depending on the strength of the coupling and the frequency of the two oscillators (8, 47). In our future work, we plan to assess the strength of the coupling and the doubling time by using both computational simulations and experiments observing both cell cycle and circadian components with bioluminescence assays. Our discovery of circadian clock-dependent synchronized mitotic cycles in Neurospora will serve as a stepping-stone for further investigations to uncover conserved principles of coupled mechanisms between the cell cycle and circadian rhythms.

Materials and Methods

Strains. Strains used for the experiments are a clock wild-type *ras-1^{bd}*;a (328-4) and three arrhythmic mutants from the laboratories of Drs. J. Dunlap and J. Loros (Dartmouth Medical School, Hanover, NH) [*ras-1^{bd}*; *frq^{ko}*;a (358-6), *ras-1^{bd};wc-1^{ko}* (S38), and *ras-1^{bd};wc-2^{ko}* (*Δwc-2*)]. Wild-type strain FGSC#2489 (Mat A) was used for the ChIP experiment. Strain *hH1-sgfp* (FGSC#9518) was obtained from the Fungal Genetics Stock Center (FGSC, University of Missouri–Kansas City) (48). *cln-1-luc*, *clb-1-luc*, and *cdc-2-luc* strains were made by integrating these reporter constructs into the *csr-1* locus as previously described (49). CLN-1^{luc}, CLB-1^{luc}, and CDC-2^{luc} translational fusion strains were made by knock-in strategies as previously described (50). The strain *clb-1-luc;frq^{ko}* is a progeny from a cross between *clb-1-luc;ras-1^{bd};A* and 358–6 (*ras-1^{bd}*; *frq^{ko}*; a). The strain *stk-29-luc;frq^{ko}* is a progeny from a cross between *stk-29-luc;ras-1^{bd};A* and 358–6 (*ras-1^{bd}*; *frq^{ko}*;a). The strain CLN-1^{luc}; *frq^{ko}* is a progeny from a cross between CLN-1^{luc};*ras-1^{bd};A* and 358–6 (*ras-1^{bd}*; *frq^{ko}*;a). The strain *hH1-sgfp;frq^{ko}* is a cross-progeny between *hH1-sgfp* (FGSC#9518) and 358–6 (*ras-1^{bd}*; *frq^{ko}*;a).

Quantitative RT-PCR. Neurospora was grown in liquid culture media containing Vogel's medium (pH 5.8) with 2% (wt/vol) glucose, 0.5% arginine, and 50 ng/mL biotin, and harvested as previously described (31). Total RNA was isolated using Tri Reagent (Molecular Research Center, Inc.), and quantitative RT-PCR (qRT-PCR) was performed as previously described (31). The *actin* mRNA is used to normalize real-time qRT-PCR data.

ChIP. ChIP was performed in a manner similar to methods previously described, with slight modifications (51, 52). One hundred-milliliter cultures of Neurospora mycelia were cross-linked with 1% formaldehyde for 15 min and then quenched with 0.1 M glycine for an additional 15 min. The Neurospora was harvested by filtration and ground with a mortar and pestle, and the tissue was added to 10 mL FA lysis buffer (0.05 M Hepes, pH 7.4/0.15 M NaCl/0.001 M EDTA/1% Triton TX-100/0.1% SDS) containing protease inhibitors (0.002 mg/mL leupeptin, 0.002 mg/mL pepstatin A, 0.001 M PMSF). To improve cell disruptions, the tissue was subjected to a single sonication at 50% power and the cellular debris was removed by centrifugation at 2500 × *g* for 10 min. A chromatin-enriched fraction then was obtained by a high-speed spin at 60,000 × *g* for 30 min. The pellet was suspended in the lysis buffer plus protease inhibitors and sonicated to an average size of 500 bp. Equal amounts of sheared chromatin were incubated with WC-2 antibody (53) plus protein A Dynabeads overnight at 4 °C with constant mixing. The beads were washed with the lysis buffer and eluted two times with 50 mL 0.1 M sodium bicarbonate and 1.0% SDS. The cross-links were reversed by incubating for 4 h at 65 °C in the presence of 0.1 M NaCl. The DNA was recovered by treatment with proteinase K for 1 h followed by a phenol/chloroform extraction, then suspended in 10 mM Tris, pH 7.5/1.0 mM EDTA. Two milliliters of the purified DNA was used in a quantitative PCR with primers specific to the *stk-29* promoter.

Bioluminescence Assay. In all experiments, Neurospora was grown at 25 °C in constant white fluorescent light (LL) overnight before being transferred into constant darkness (DD) for time-course experiments. For bioluminescence assays, we used standard race tubes containing Vogel's medium (pH 5.8) with 0.1% glucose, 0.17% arginine, 50 ng/mL biotin, 1.5% (wt/vol) agar, and 12.5 μM luciferin (Fig. 2). In vivo luciferase activity was collected for 10 min every hour with a PIXIS CCD camera from Princeton Instruments controlled by WinView/32 software from Roper Scientific. A 90-min pulse of white fluorescent light (80 μmol photons·m^{-2}·s^{-1}) was given at indicated time points for phase-shift experiments, and in vivo luciferase activity was collected for 10 min every 2 h.

Microscopy. For microscopy experiments, Neurospora conidia suspensions were grown in 500-mL baffled flasks in liquid culture media containing Vogel's medium (pH 5.8) with 2% (wt/vol) glucose, 0.5% arginine, and 50 ng/mL biotin. Neurospora was grown at 25 °C in constant white fluorescent light (LL) overnight before being transferred into constant dark (DD) for time-course experiments. Samples were grown on a shaker at 125 rpm. Random samples of mycelia were collected and fixed in 2% (wt/vol) paraformaldehyde/PBS at indicated time points and observed under a confocal fluorescence microscope (Zeiss LSM710). Two to three slides were prepared from each time point, and four to six images of mycelia were captured from each slide. Nuclei from each image were analyzed to calculate the average number of nuclei undergoing mitosis.

ACKNOWLEDGMENTS. We thank P. Stambrook, M. Montrose, N. Horsemen, K. Lee, and C. H. Chen for discussions. We thank S. Yoo, S. Moon, D. Ruter, and S. Kim for technical assistance. We thank C. Closson at the Live Microscopy Core for his help with confocal microscopy, and the Fungal Genetics Stock Center for providing the *hH1-sgfp* strain (FGSC#9518) (48). We are pleased to acknowledge use of materials generated by Grant P01 GM0668087, "Functional Analysis of a Model Filamentous Fungus" (54). C.I.H. was supported by Department of Interior Grant D12AP00005 and startup funds from the Department of Molecular and Cellular Physiology, University of Cincinnati. L.F.L. was supported by Fondo Nacional de Desarrollo Cientifico y Tecnologico 1090513. W.J.B. is supported by National Institutes of Health Grant R01 GM101378 and is a member of the National Institute on Environmental Health Sciences Center for Environmental Exposure and Disease (P30 ES005022).

1. Fu L, Pelicano H, Liu J, Huang P, Lee C (2002) The circadian gene Period2 plays an important role in tumor suppression and DNA damage response in vivo. *Cell* 111(1):41–50.
2. Green CB, Takahashi JS, Bass J (2008) The meter of metabolism. *Cell* 134(5):728–742.
3. Panda S, et al. (2002) Coordinated transcription of key pathways in the mouse by the circadian clock. *Cell* 109(3):307–320.
4. Edmunds LN, Jr., Funch RR (1969) Circadian rhythm of cell division in Euglena: Effects of random illumination regimen. *Science* 165(3892):500–503.
5. Matsuo T, et al. (2003) Control mechanism of the circadian clock for timing of cell division in vivo. *Science* 302(5643):255–259.
6. Sweeney BM, Hastings JW (1958) Rhythmic cell division in populations of Gonyaulax polyedra. *J Eukaryot Microbiol* 5:217–224.
7. Yang Q, Pando BF, Dong G, Golden SS, van Oudenaarden A (2010) Circadian gating of the cell cycle revealed in single cyanobacterial cells. *Science* 327(5972):1522–1526.
8. Zámborszky J, Hong CI, Csikász Nagy A (2007) Computational analysis of mammalian cell division gated by a circadian clock: Quantized cell cycles and cell size control. *J Biol Rhythms* 22(6):542–553.
9. Yeom M, Pendergast JS, Ohmiya Y, Yamazaki S (2010) Circadian-independent cell mitosis in immortalized fibroblasts. *Proc Natl Acad Sci USA* 107(21):9665–9670.
10. Dunlap JC, et al. (2007) A circadian clock in Neurospora: How genes and proteins cooperate to produce a sustained, entrainable, and compensated biological oscillator with a period of about a day. *Cold Spring Harb Symp Quant Biol* 72:57–68.
11. Liu Y, Bell-Pedersen D (2006) Circadian rhythms in Neurospora crassa and other filamentous fungi. *Eukaryot Cell* 5(8):1184–1193.
12. Aronson BD, Johnson KA, Loros JJ, Dunlap JC (1994) Negative feedback defining a circadian clock: Autoregulation of the clock gene frequency. *Science* 263(5153):1578–1584.
13. Cheng P, He Q, He Q, Wang L, Liu Y (2005) Regulation of the Neurospora circadian clock by an RNA helicase. *Genes Dev* 19(2):234–241.
14. Cha J, Chang SS, Huang G, Cheng P, Liu Y (2008) Control of WHITE COLLAR localization by phosphorylation is a critical step in the circadian negative feedback process. *EMBO J* 27(24):3246–3255.

15. Hong CI, Ruoff P, Loros JJ, Dunlap JC (2008) Closing the circadian negative feedback loop: FRQ-dependent clearance of WC-1 from the nucleus. *Genes Dev* 22(22): 3196–3204.
16. Schafmeier T, et al. (2008) Circadian activity and abundance rhythms of the Neurospora clock transcription factor WCC associated with rapid nucleo-cytoplasmic shuttling. *Genes Dev* 22(24):3397–3402.
17. Baker CL, Kettenbach AN, Loros JJ, Gerber SA, Dunlap JC (2009) Quantitative proteomics reveals a dynamic interactome and phase-specific phosphorylation in the Neurospora circadian clock. *Mol Cell* 34(3):354–363.
18. Querfurth C, et al. (2011) Circadian conformational change of the Neurospora clock protein FREQUENCY triggered by clustered hyperphosphorylation of a basic domain. *Mol Cell* 43(5):713–722.
19. Tang CT, et al. (2009) Setting the pace of the Neurospora circadian clock by multiple independent FRQ phosphorylation events. *Proc Natl Acad Sci USA* 106(26): 10722–10727.
20. Gladfelter AS (2006) Nuclear anarchy: Asynchronous mitosis in multinucleated fungal hyphae. *Curr Opin Microbiol* 9(6):547–552.
21. Roca MG, Kuo HC, Lichius A, Freitag M, Read ND (2010) Nuclear dynamics, mitosis, and the cytoskeleton during the early stages of colony initiation in Neurospora crassa. *Eukaryot Cell* 9(8):1171–1183.
22. Serna L, Stadler D (1978) Nuclear division cycle in germinating conidia of Neurospora crassa. *J Bacteriol* 136(1):341–351.
23. Rosenberger RF, Kessel M (1967) Synchrony of nuclear replication in individual hyphae of Aspergillus nidulans. *J Bacteriol* 94(5):1464–1469.
24. Freitag M, Hickey PC, Raju NB, Selker EU, Read ND (2004) GFP as a tool to analyze the organization, dynamics and function of nuclei and microtubules in Neurospora crassa. *Fungal Genet Biol* 41(10):897–910.
25. Galagan JE, et al. (2003) The genome sequence of the filamentous fungus Neurospora crassa. *Nature* 422(6934):859–868.
26. Borkovich KA, et al. (2004) Lessons from the genome sequence of Neurospora crassa: Tracing the path from genomic blueprint to multicellular organism. *Microbiol Mol Biol Rev* 68(1):1–108.
27. Nurse P (1990) Universal control mechanism regulating onset of M-phase. *Nature* 344(6266):503–508.
28. Csikász-Nagy A, Battogtokh D, Chen KC, Novák B, Tyson JJ (2006) Analysis of a generic model of eukaryotic cell-cycle regulation. *Biophys J* 90(12):4361–4379.
29. Froehlich AC, Liu Y, Loros JJ, Dunlap JC (2002) White Collar-1, a circadian blue light photoreceptor, binding to the frequency promoter. *Science* 297(5582):815–819.
30. He Q, et al. (2002) White collar-1, a DNA binding transcription factor and a light sensor. *Science* 297(5582):840–843.
31. Chen CH, Ringelberg CS, Gross RH, Dunlap JC, Loros JJ (2009) Genome-wide analysis of light-inducible responses reveals hierarchical light signalling in Neurospora. *EMBO J* 28(8):1029–1042.
32. Gooch VD, et al. (2008) Fully codon-optimized luciferase uncovers novel temperature characteristics of the Neurospora clock. *Eukaryot Cell* 7(1):28–37.
33. Tyson JJ, Novak B (2001) Regulation of the eukaryotic cell cycle: Molecular antagonism, hysteresis, and irreversible transitions. *J Theor Biol* 210(2):249–263.
34. Larrondo LF, Loros JJ, Dunlap JC (2012) High-resolution spatiotemporal analysis of gene expression in real time: In vivo analysis of circadian rhythms in Neurospora crassa using a FREQUENCY-luciferase translational reporter. *Fungal Genet Biol* 49(9): 681–683.
35. Spellman PT, et al. (1998) Comprehensive identification of cell cycle-regulated genes of the yeast Saccharomyces cerevisiae by microarray hybridization. *Mol Biol Cell* 9(12): 3273–3297.
36. Hendzel MJ, et al. (1997) Mitosis-specific phosphorylation of histone H3 initiates primarily within pericentromeric heterochromatin during G2 and spreads in an ordered fashion coincident with mitotic chromosome condensation. *Chromosoma* 106(6):348–360.
37. Plikus MV, et al. (2013) Local circadian clock gates cell cycle progression of transient amplifying cells during regenerative hair cycling. *Proc Natl Acad Sci USA* 110(23): E2106–E2115.
38. Dunlap JC (1999) Molecular bases for circadian clocks. *Cell* 96(2):271–290.
39. Gamsby JJ, Loros JJ, Dunlap JC (2009) A phylogenetically conserved DNA damage response resets the circadian clock. *J Biol Rhythms* 24(3):193–202.
40. Gery S, et al. (2006) The circadian gene per1 plays an important role in cell growth and DNA damage control in human cancer cells. *Mol Cell* 22(3):375–382.
41. Hong CI, Zámborszky J, Csikász-Nagy A (2009) Minimum criteria for DNA damage-induced phase advances in circadian rhythms. *PLOS Comput Biol* 5(5):e1000384.
42. Oklejewicz M, et al. (2008) Phase resetting of the mammalian circadian clock by DNA damage. *Curr Biol* 18(4):286–291.
43. Pregueiro AM, Liu Q, Baker CL, Dunlap JC, Loros JJ (2006) The Neurospora checkpoint kinase 2: A regulatory link between the circadian and cell cycles. *Science* 313(5787): 644–649.
44. Smith KM, et al. (2010) Transcription factors in light and circadian clock signaling networks revealed by genomewide mapping of direct targets for neurospora white collar complex. *Eukaryot Cell* 9(10):1549–1556.
45. Dong W, et al. (2008) Systems biology of the clock in Neurospora crassa. *PLoS One* 3(8):e3105.
46. Martegani E, Levi M, Trezzi F, Alberghina L (1980) Nuclear division cycle in Neurospora crassa hyphae under different growth conditions. *J Bacteriol* 142(1):268–275.
47. Gérard C, Goldbeter A (2012) Entrainment of the mammalian cell cycle by the circadian clock: Modeling two coupled cellular rhythms. *PLOS Comput Biol* 8(5):e1002516.
48. McCluskey K, Wiest A, Plamann M (2010) The Fungal Genetics Stock Center: A repository for 50 years of fungal genetics research. *J Biosci* 35(1):119–126.
49. Chen CH, DeMay BS, Gladfelter AS, Dunlap JC, Loros JJ (2010) Physical interaction between VIVID and white collar complex regulates photoadaptation in Neurospora. *Proc Natl Acad Sci USA* 107(38):16715–16720.
50. Larrondo LF, Colot HV, Baker CL, Loros JJ, Dunlap JC (2009) Fungal functional genomics: Tunable knockout-knock-in expression and tagging strategies. *Eukaryot Cell* 8(5):800–804.
51. Belden WJ, Lewis ZA, Selker EU, Loros JJ, Dunlap JC (2011) CHD1 remodels chromatin and influences transient DNA methylation at the clock gene frequency. *PLoS Genet* 7(7):e1002166.
52. Belden WJ, Loros JJ, Dunlap JC (2007) Execution of the circadian negative feedback loop in Neurospora requires the ATP-dependent chromatin-remodeling enzyme CLOCKSWITCH. *Mol Cell* 25(4):587–600.
53. Denault DL, Loros JJ, Dunlap JC (2001) WC-2 mediates WC-1-FRQ interaction within the PAS protein-linked circadian feedback loop of Neurospora. *EMBO J* 20(1-2): 109–117.
54. Colot HV, et al. (2006) A high-throughput gene knockout procedure for Neurospora reveals functions for multiple transcription factors. *Proc Natl Acad Sci USA* 103(27): 10352–10357.